Supporting information

Rational Synthesis of Pd Dual-Atom Catalysts via Molecular Precursor Engineering for Selective Hydrogenation

Kai Zhang[1], Chunyi Yu[2,3], Shang Han[1], Yang Wang[1], Yang Liu[1], Zhi-Wei Xing[4], Lifeng Ding[2]*, and Lin-Bing Sun[1]*

[1]State Key Laboratory of Materials-Oriented Chemical Engineering, Jiangsu National Synergetic Innovation Center for Advanced Materials (SICAM), College of Chemical Engineering, Nanjing Tech University, Nanjing 211816, China;

[2]Department of Chemistry and Materials Science, Advanced Materials Research Center, School of Science, Xi'an Jiaotong-Liverpool University, Suzhou 215123, China；

[3]School of Materials Science and Engineering, Hainan University, Haikou 570228, PR China；

[4]Zhejiang Provincial Key Laboratory of Advanced Chemical Engineering Manufacture Technology, College of Chemical and Biological Engineering, Zhejiang University, Hangzhou 310027, China.

*Corresponding author. Email: lbsun@njtech.edu.cn; Lifeng.Ding@xjtlu.edu.cn

Experimental Section

Chemicals

Graphene oxide was purchased from Institute of Coal Chemistry, Chinese Academy of Science. The chemicals (en)$Pd(NO_3)_2$, 4,4'-bipyridine, phenylacetylene, styrene and ethylbenzene were purchased from Shanghai Ling Feng Chemical Reagent Co., Ltd. Ethanol (EtOH) was purchased from Sinopharm Chemical Reagent Co., Ltd.

Synthesis of Pd_4L_4

Pd_4L_4 was prepared according to the previous report.[1] A typical Pd_4L_4 solution is obtained by adding a methanol solution (4 mL) of 4,4'-bipyridine (0.5 mmol) to a methanol-water (1:1, 4 mL) solution of (en)$Pd(NO_3)_2$ (0.5 mmol) at ambient temperature and stirring for 30 minutes.

Synthesis of Pd-NPC

The reference sample with Pd nanoparticles was synthesized as follows. The Pd salt aqueous solution was obtained by accurately weighing 2.9 mg of (en)$Pd(NO_3)_2$ and 5 mL of water. The solution was added to 16.5 mL of GO aqueous solution (14 mg/mL) and stirred for 24 h. The subsequent operation is the same as the above Pd-DAC synthesis step. The obtained catalyst was named Pd-NPC. The Pd content after annealing was tested by inductively coupled plasma (ICP), and the loading was 0.68 %.

Synthesis of the Pd Single-Atom Catalyst Pd_1/NC

Pd_1/NC was synthesized by the reported method.[2] Firstly, $Pd(acac)_2$ (68.607 mg, 0.225 mmol) and $Zn(NO_3)_2.6H_2O$ (1.069 g, 3.6 mmol) were dissolved in a 30 mL of methanol solution, followed by the addition of a 10 mL of methanol solution containing 2-methylimidazole(1.161 g, 14.2 mmol), then stirred vigorously for 5 minutes, The mixture solution was allowed to age for 20 hours at room temperature. The solid product was collected by centrifugation and washed with methanol four times. The product was dried at 70°C in a vacuum oven to obtain the $Pd(acac)_2$@ZIF-8 compound. Secondly, $Pd(acac)_2$@ZIF-8 was placed in a tubular furnace

and heated at 900 ºC with a heating rate of 5 ºC/min in argon atmosphere for 3 hours and tubular furnace was cooled to room temperature. Finally, solid product was collected to obtain Pd_1/NC.

DFT Calculations

The edge-functionalized graphene oxide (GO) model was generated using the web-based computational tool. Structural parameters were calibrated according to experimental characterization data, with the oxygen content rigorously constrained to around 30 weights% (wt%) to replicate the oxidation degree of synthesized GO samples. The functional group distribution was configured with a 1:1 molar ratio between hydroxyl (-OH) and carboxyl (-COOH) groups, adhering to spectroscopic observations. The 3D visualization of crystal structures and charge distributions was carried out using VESTA[2], which supports volumetric data and crystal morphology rendering. Spin-polarized density functional theory (DFT) calculations were carried out using the Vienna ab initio Simulation Package (VASP) version 6.4.2,[3, 4] employing a plane-wave basis set with projector-augmented wave (PAW) pseudopotential.[5] The Perdew-Burke-Ernzerhof (PBE) exchange-correlation functional[6] was adopted, supplemented with Grimme's DFT-D311 dispersion correction to account for van der Waals interactions.

Structural optimizations were performed under constant lattice parameters with atomic positions relaxed using the conjugate gradient algorithm. Convergence criteria were set to energy changes less than 1×10^{-5} eV between successive electronic steps and maximum ionic forces less than 0.02 eV·Å^{-1} on all atoms. A plane-wave kinetic energy cutoff of 450 eV was applied throughout the calculations. For Brillouin zone integration, a Γ-centered 1×1×1 k-point mesh was implemented with Gaussian smearing (σ=0.05 eV) to accelerate electronic convergence. The values of the differential charge density isosurfaces in Figures 1b and 1c are identical, both set to 0.001 e/bohr^3.

Catalytic Evaluation

The selective hydrogenation of phenylacetylene was carried out in a 10 ml Schlenk glass vessel tube with a magnetic stirrer. In the vessel tube, 10 mg of catalyst, 0.91 mmol of substrate were

added and mixed well, and the air inside the vessel tube was removed by purging with hydrogen more than 5 times, and finally an external hydrogen balloon was connected. The reaction setup was heated at a constant temperature in a water bath at 30 °C. The liquid product was separated by filtration and used for analysis by gas chromatography (GC, Agilent 7890A) equipped with a flame ionization detector. Phenylacetylene conversion and product selectivity are defined as follows:

$$\text{Conversion (\%)} = \frac{phenylacetylene\ feed - phenylacetylene\ residue}{phenylacetylene\ feed} \times 100\%$$

$$\text{Selectivity (\%)} = \frac{styrene\ product}{phenylacetylene\ feed - phenylacetylene\ residue} \times 100\%$$

After each reaction, the catalyst was separated from the reaction solution by centrifugation, and then the reaction solution was removed. Finally, the catalyst was vacuum dried at 80 °C, overnight, and activated at 620 °C. The obtained catalyst is subjected to the next cycle under the same conditions as above.

Materials Characterization

X-ray diffraction (XRD) patterns were recorded on a Bruker D8 Avance diffractometer operated at 40 kV and 40 mA using a Cu Kα radiation (λ=0.15406 nm) at a step width of 2° min^{-1}. Fourier transform infrared (FT-IR) spectra were tested with a Nicolet Nexus 470 spectrometer at the spectra resolution of 2 cm^{-1}. X-ray photoelectron spectroscopy (XPS) analysis was performed using an ESCALAB-220I-XL (Thermo-Electron, VG Company) device equipped with an Al Kα X-ray source (hv = 1486.6 eV) at 10 kV and 35 mA, and the binding energies were referred to C 1s at 284.8 eV. The morphology of the materials was identified by transmission electron microscopy (TEM, JEOL 2100F) operated at an accelerating voltage of 200 kV and aberration-corrected high-angle annular dark-field scanning transmission electron microscopy (HAADF-STEM, Titan Cubed Themis G2 300). Pd content was tested by Perkin Elmer OPTIMA7000DV inductively coupling plasma (ICP). Raman spectra were recorded by Horiba (Labram HR800) with a 532 nm excitation laser. In situ diffuse reflectance Fourier transform infrared spectroscopy (DRIFTS) experiments were conducted on a Nicolet iS50 Fourier transform infrared spectrometer (FT-IR). The X-ray absorption near

edge structure (XANES) of Pd K edge were performed at the BL11B beamline of Shanghai Synchrotron Radiation Facility (SSRF). The samples were ground and daubed uniformly on the unique double-sided carbon adhesive tape, the data were collected in fluorescence mode and the curves are normalized. The EXAFS spectroscopy measured with FLY (fluorescence yield) mode was numerically fitted by the real space multiple scattering program of FEFF5. Note: $S_0^2$is the amplitude reduction factor, according to the experimental EXAFS fitted with of Pd foil reference by fixing CN as the known crystallographic value. ARTEMIS evaluates a variety of statistical parameters relevant to the evaluation of the fit. For example, E_0 is rarely more than 10 eV or less than -10 eV, that $S_0^2$and σ^2should never be negative. σ^2value in the range between 0.001 and 0.01 will not be got a penalty. Artemis software thinks any fit which *R*-factor has 2% or less misfit between data and theory is not assessed a penalty. The errors were automatically generated by the Athena and Artemis software. The TEM and HAADF-STEM characterizations reflect the local information of the sample and demonstrate the atomic level dispersion of the metal at the microscopic level with the most direct picture. The XANES characterizations show the overall information of the sample and prove the atomic dispersion of the metal at the macroscopic level. The combination of these characterizations gives comprehensive information on metal dispersion.

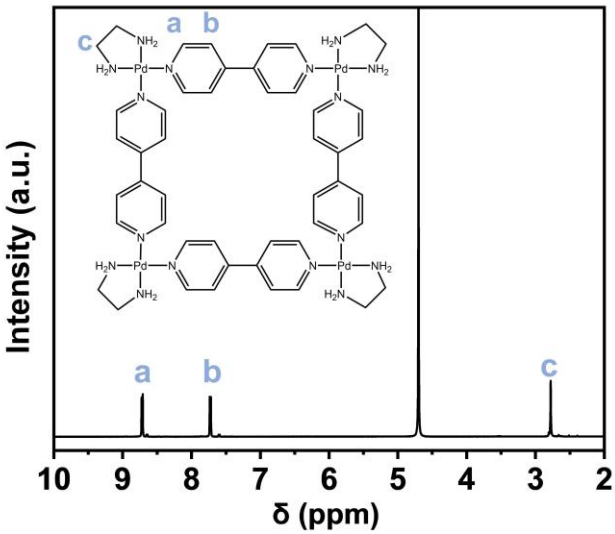

Figure S1. Liquid-state ^{1}H NMR Spectrum of Pd_4L_4, where the peaks labeled a, b, and c correspond to protons in different chemical environments.

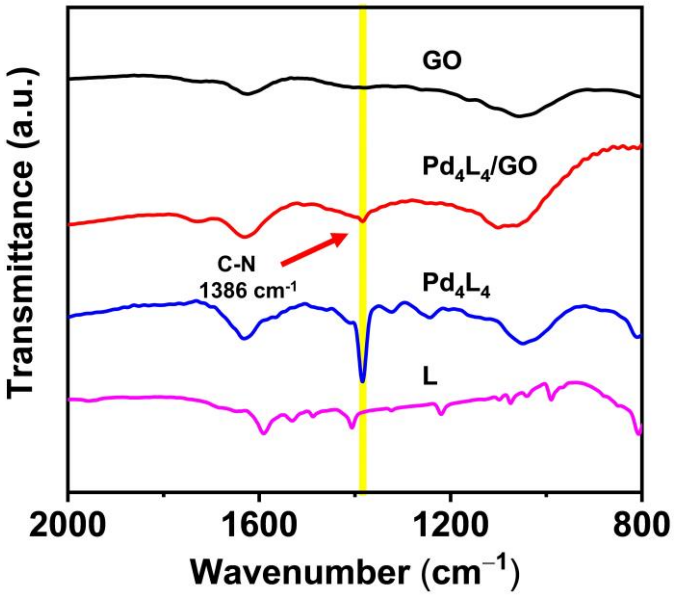

Figure S2. IR spectra of GO, Pd_4L_4/GO, Pd_4L_4, and L. The spectra reveal distinct C-N stretching vibration peaks at 1386 cm^{-1} for both Pd_4L_4 and Pd_4L_4/GO.

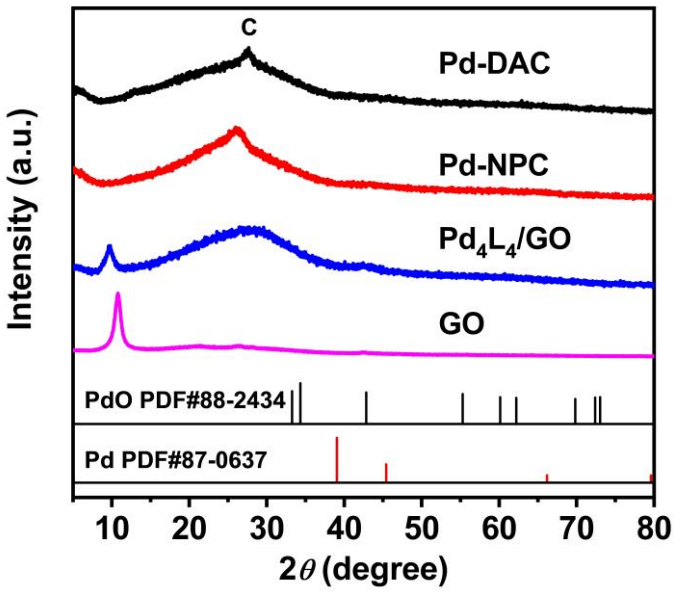

Figure S3. XRD patterns of Pd_4L_4/GO, GO, Pd-DAC and Pd-NPC, in which no characteristic diffraction peaks of Pd or PdO crystalline phases were observed, and the diffraction peak at ~26° is assigned to the (002) crystal plane of carbon.

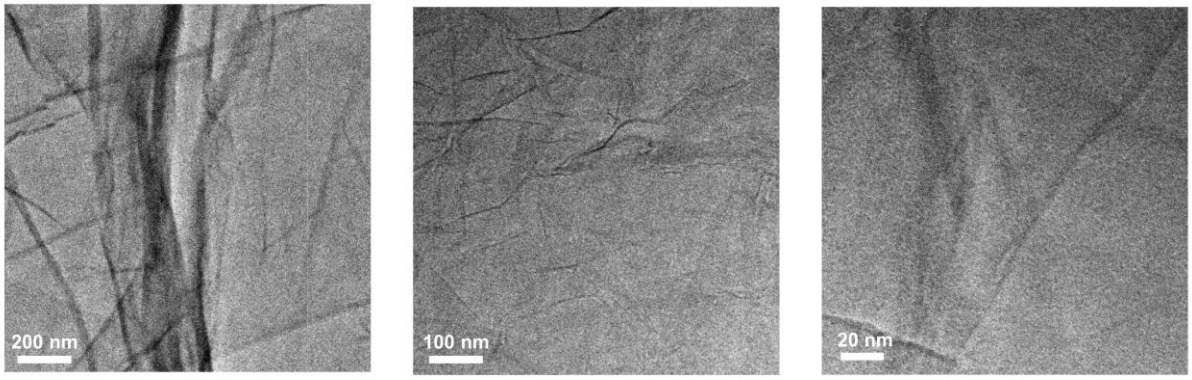

Figure S4. TEM images of Pd-DAC at different magnifications.

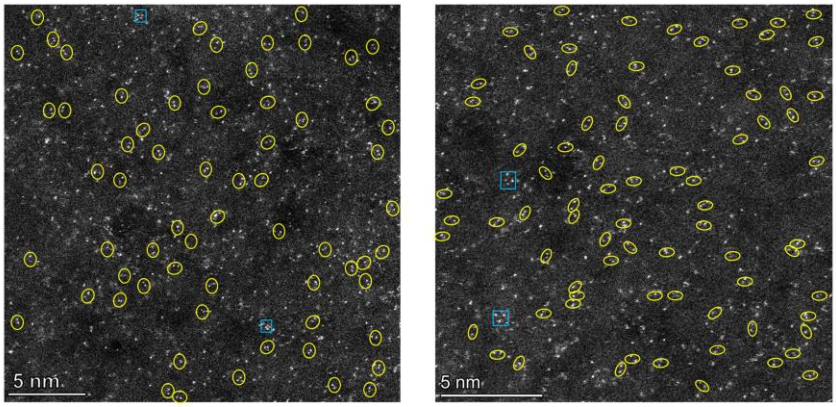

Figure S5. Spherical aberration corrected HAAFD-STEM images of Pd-DAC at different areas.

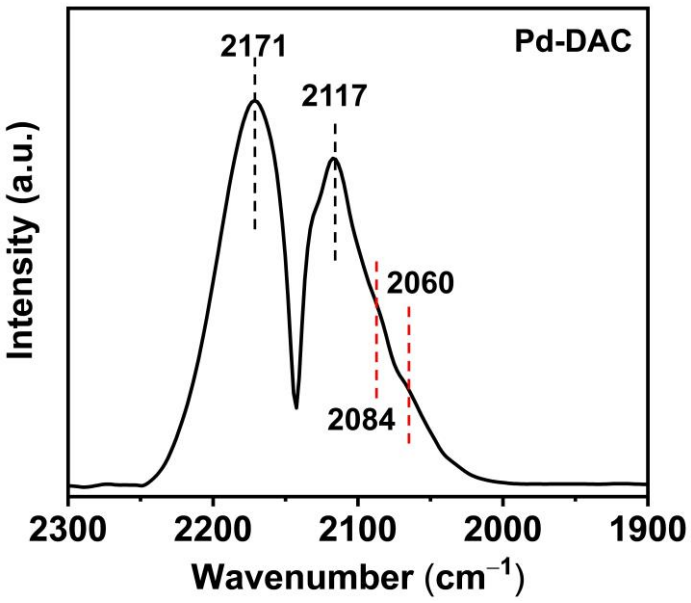

Figure S6. In-situ CO-DRIFTS spectrum of Pd-DAC.

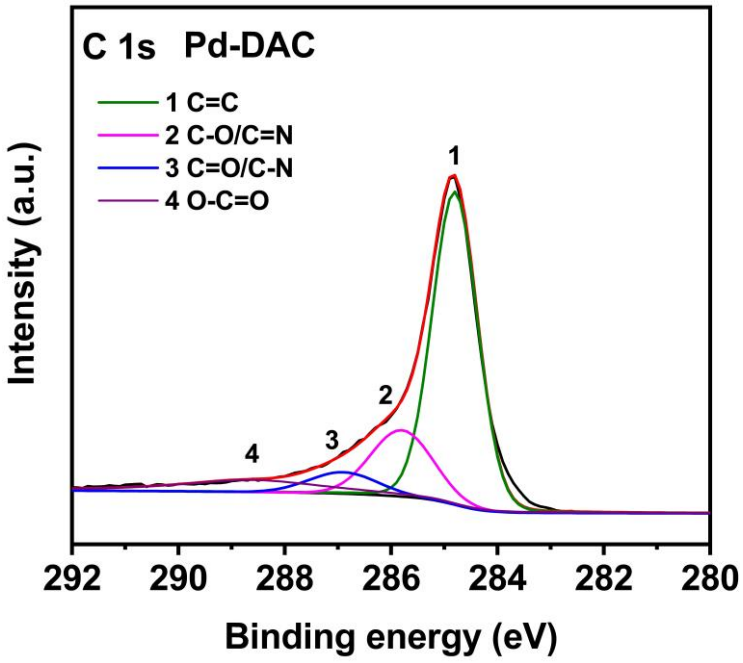

Figure S7. The XPS spectrum of C 1s in Pd-DAC.

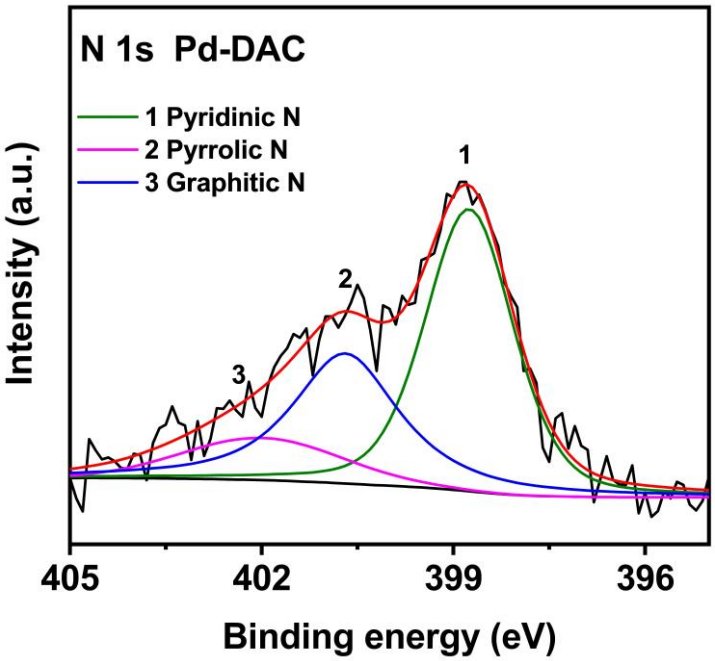

Figure S8. The XPS spectrum of N 1s in Pd-DAC.

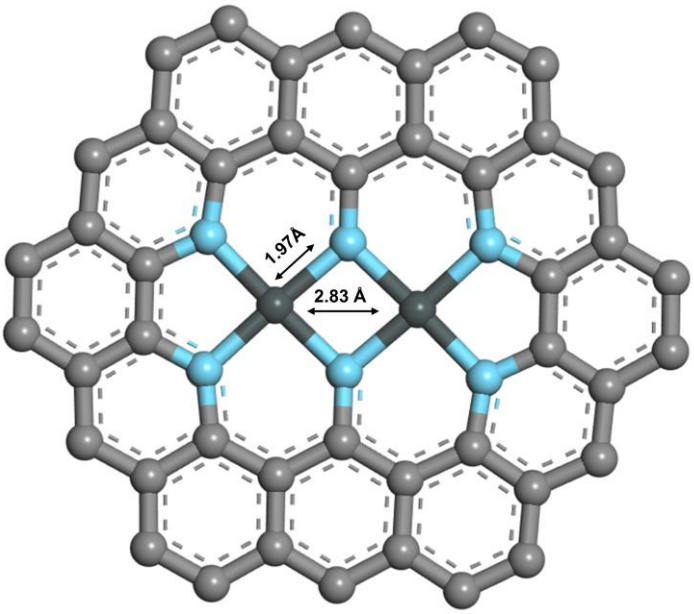

Figure S9. Coordination configuration of Pd-DAC.

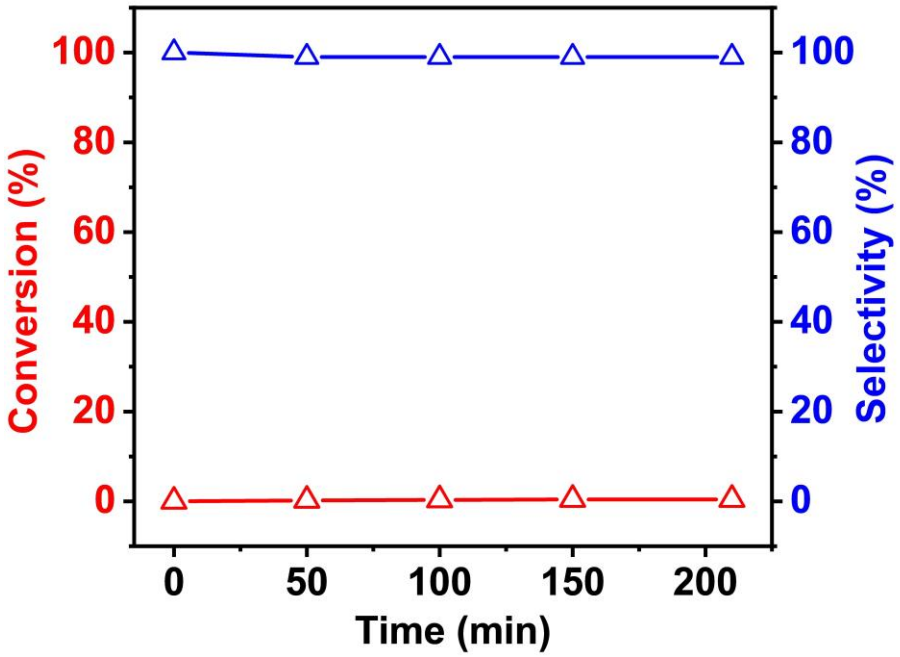

Figure S10. Catalytic performance of GO for selective hydrogenation of phenylacetylene to styrene (reaction conditions: phenylacetylene, 0.91 mmol, C_2H_5OH, 6 mL, H_2 balloon, 303 K, 3.5 h).

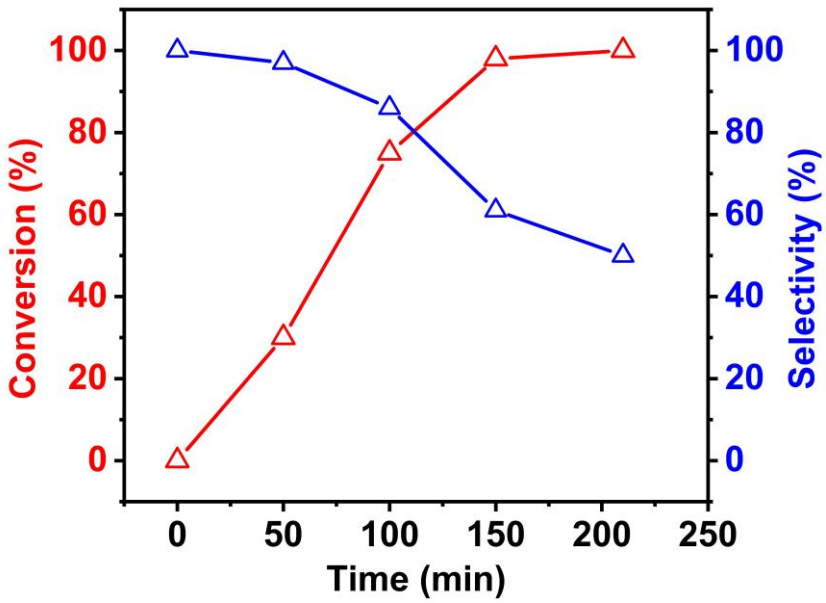

Figure S11. Catalytic performance of Pd-NPC for selective hydrogenation of phenylacetylene to styrene (reaction conditions: phenylacetylene, 0.91 mmol, C_2H_5OH, 6 mL, H_2 balloon, 303 K, 3.5 h).

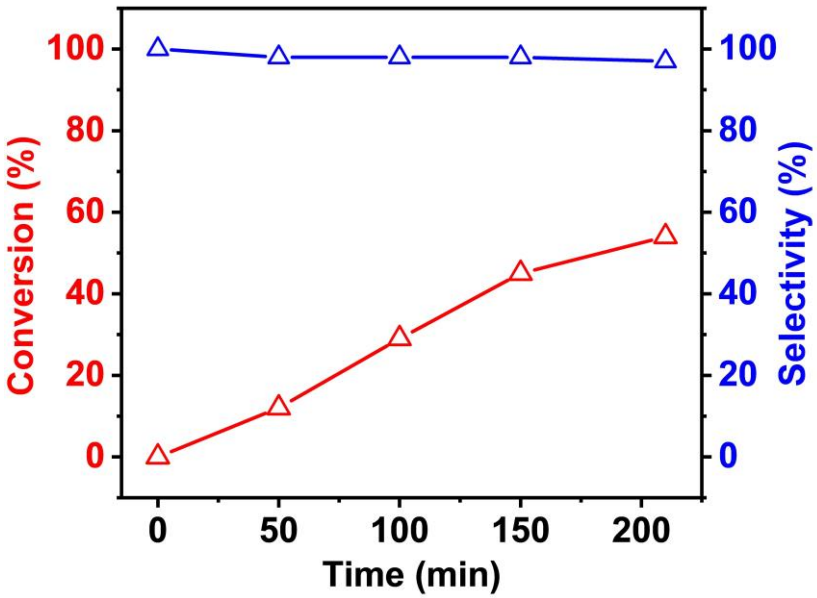

Figure S12. Catalytic performance of commercial Lindlar catalyst for selective hydrogenation of phenylacetylene to styrene. (reaction conditions: phenylacetylene, 0.91 mmol, C_2H_5OH, 6 mL, H_2 balloon, 303 K, 3.5 h).

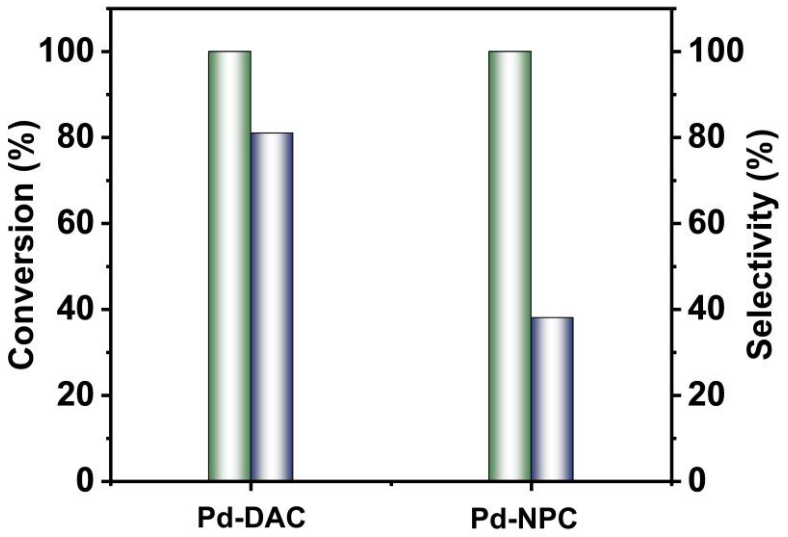

Figure S13. Catalytic performance of Pd-DAC and Pd-NPC in the selective hydrogenation of phenylacetylene to styrene for extended time to 5.5 h.

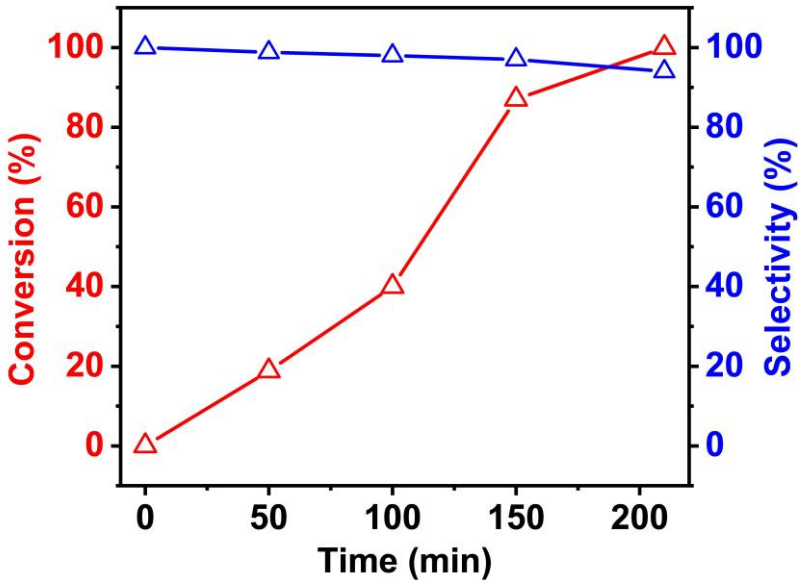

Figure S14. Catalytic activity and selectivity data of the re-synthesized Pd-DAC sample. (Pd content determined by ICP: 0.70 wt%; reaction conditions: phenylacetylene, 0.91 mmol, C_2H_5OH, 6 mL, H_2 balloon, 303 K, 3.5 h).

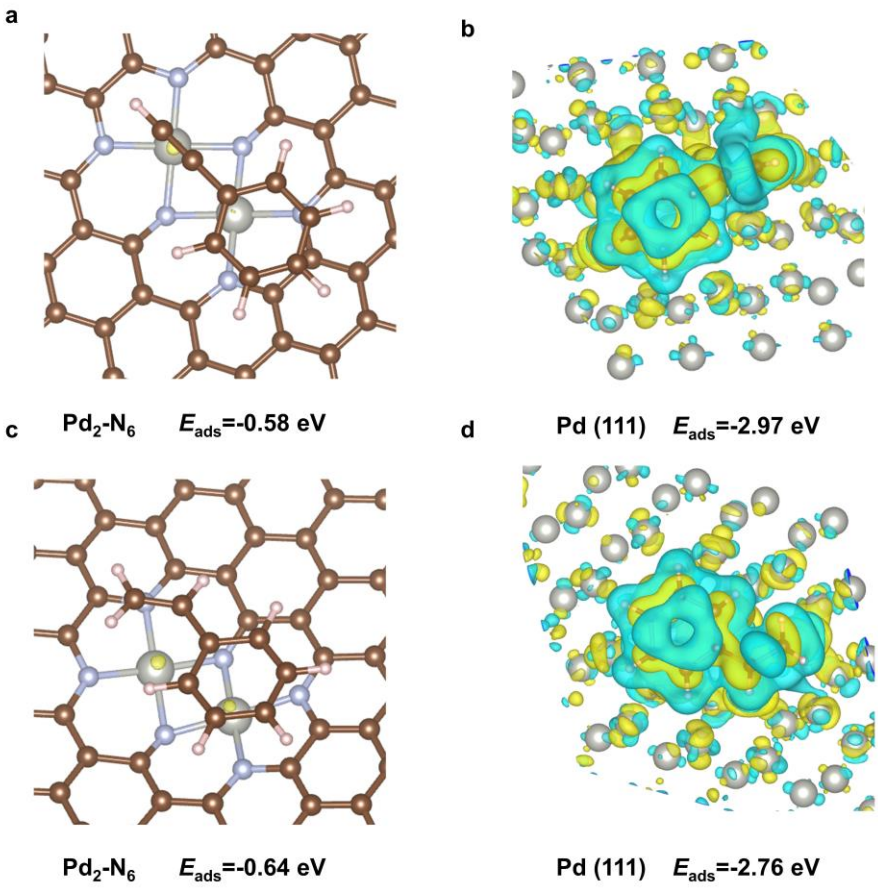

Figure S15. (a) Electron density difference at the interface between the Pd_2-N_6 or (b) Pd (111) surface and the phenylacetylene molecule.(c) Electron density difference at the interface between the Pd_2-N_6 or (d) Pd(111) surface and the styrene molecule. The values of the differential charge density isosurfaces are identical, both set to 0.001 e/bohr^3.

Table S1. Structural parameters extracted from the Pd K-edge EXAFS fitting (S_0^2=0.83)

Sample	Shell	CN	*R* (Å)	$\sigma^2(10^{-3}Å^2)$	ΔE_0 (eV)	R factor
Pd-DAC	Pd-N	3.9	1.98	9.83	6.44	0.0652
	Pd-Pd	1.4	2.82	10.27		
Pd-NPC	Pd-N	3.9	2.05	3.01	0.91	0.0212
	Pd-Pd	8.2	2.77	8.49		
Pd foil	Pd-Pd	12*	2.76	5.88	1.25	0.0013
PdO	Pd-O	4*	2.03	2.55	3.92	0.0164
	Pd-Pd	4*	3.06	1.41		
	Pd-Pd	8*	3.42	5.30		

Note: S_0^2 is the amplitude reduction factor; CN is the coordination number; *R* is interatomic distance (the bond length between central atoms and surrounding coordination atoms); σ^2 is Debye-Waller factor (a measure of thermal and static disorder in absorber-scatterer distances); ΔE_0 is edge-energy shift (the difference between the zero kinetic energy value of the sample and that of the theoretical model); *R* factor is used to value the goodness of the fitting.

*The value was fixed during EXAFS fitting, based on the known structure of Pd foil and PdO. Error bounds that characterize the structural parameters obtained by EXAFS spectroscopy were estimated as N ± 20 %; *R* ± 1 %; σ^2 ± 20 %; ΔE_0 ± 20 %.

Table S2. Comparison of catalytic performance of different catalysts for the semi-hydrogenation of phenylacetylene

Catalyst	Time (h)	T (°C)	P (bar)	Con. (%)	Sel. (%)	TOF (h^{-1})	Ref.
Pd-DAC	3.5	30	1	100	93	411	This Work
Ru_3@ZIF-8	5	80	40	47	97	6	7
Ni@NC-800	4	110	10	97	94	5	8
Au/CeO_2	12	25	30	98	97	20	9
Pt@Y-SOD	5	150	8	50	95	310	10
NiCu/NMO	5	100	4	100	70	19	11
Pd_1/NC-PHF	5	20	1	74	93	139	12
Pd(0)-AmP-HSNs	2	25	1	93	89	106	13
Pd+PEI(L)@HSS	4	30	1	99	84	27	14
Pd/P-PCFs	2	20	3	87	73	332	15
PdNCs@NCM	5	25	1	99	95	396	16
Pd@PDA@PUF	7	25	1	91	95	376	17
PdC_x@S-1	4	25	2	100	99	320	18
Pd/PPh_3@FDU-12	0.7	25	1	92	94	560	19
UiO67@Pd@UiO-66	0.4	25	5	100	92	258	20
Pd_1-Fe/Fe_2O_3(012)	1.4	30	15	>99	>99	379	21
Pd_1-Cu	3.5	25	6.5	90	94	113	22
Pd&ZnO@carbon	1.5	30	1	96	99	653	23
Pd_3Fe/meso S-C	3.2	25	6.5	100	97	335	24

References

1. M. Fujita, J. Yazaki and K. Ogura, *J. Am. Chem. Soc.*, 1990, **112**, 5645-5647.
2. Z. Li, Y. Chen, S. Ji, Y. Tang, W. Chen, A. Li, J. Zhao, Y. Xiong, Y. Wu, Y. Gong, T. Yao, W. Liu, L. Zheng, J. Dong, Y. Wang, Z. Zhuang, W. Xing, C. T. He, C. Peng, W. C. Cheong, Q. Li, M. Zhang, Z. Chen, N. Fu, X. Gao, W. Zhu, J. Wan, J. Zhang, L. Gu, S. Wei, P. Hu, J. Luo, J. Li, C. Chen, Q. Peng, X. Duan, Y. Huang, X. M. Chen, D. Wang and Y. Li, *Nat Chem.*, 2020, **12**, 764-772.
3. G. Kresse and J. Furthmüller, *Phys. Rev. B*, 1996, **54**, 11169-11186.
4. G. Kresse and J. Furthmüller, *Comput. Mater. Sci.*, 1996, **6**, 15-50.
5. G. Kresse and D. Joubert, *Phys. Rev. B*, 1999, **59**, 1758-1775.
6. J. P. Perdew, K. Burke and M. Ernzerhof, *Phys. Rev. Lett.*, 1996, **77**, 3865-3868.
7. S. Ji, Y. Chen, S. Zhao, W. Chen, L. Shi, Y. Wang, J. Dong, Z. Li, F. Li, C. Chen, Q. Peng, J. Li, D. Wang and Y. Li, *Angew. Chem. Int. Ed.*, 2019, **58**, 4271-4275.
8. X. Wang, T. Song, G. Fu and Y. Yang, *ACS Catal.*, 2023, **13**, 11634-11643.
9. T. Mitsudome, M. Yamamoto, Z. Maeno, T. Mizugaki, K. Jitsukawa and K. Kaneda, *J. Am. Chem. Soc.*, 2015, **137**, 13452-13455.
10. X. Zhang, Z. Li, W. Pei, G. Li, W. Liu, P. Du, Z. Wang, Z. Qin, H. Qi, X. Liu, S. Zhou, J. Zhao, B. Yang and W. Shen, *ACS Catal.*, 2022, **12**, 3634-3643.
11. Y. Liu, J. Zhao, J. Feng, Y. He, Y. Du and D. Li, *J. Catal.*, 2018, **359**, 251-260.
12. S. Li, G. Yue, H. Li, J. Liu, L. Hou, N. Wang, C. Cao, Z. Cui and Y. Zhao, *Chem. Eng. J.*, 2023, **454**, 140031.
13. O. Verho, H. Zheng, K. P. J. Gustafson, A. Nagendiran, X. Zou and J. E. Bäckvall, *ChemCatChem*, 2016, **8**, 773-778.
14. Y. Kuwahara, H. Kango and H. Yamashita, *ACS Catal.*, 2019, **9**, 1993-2006.
15. W. Yu, Z. Xin, S. Niu, T.-W. Lin, W. Guo, Y. Xie, Y. Wu, X. Ji and L. Shao, *Catal. Sci. Technol.*, 2017, **7**, 4934-4939.
16. X. Li, Y. Pan, H. Yi, J. Hu, D. Yang, F. Lv, W. Li, J. Zhou, X. Wu, A. Lei and L. Zhang, *ACS Catal.*, 2019, **9**, 4632-4641.
17. H. Peng, X. Zhang, V. Papaefthimiou, C. Pham-Huu and V. Ritleng, *Green Chem.*, 2023,

25, 264-279.

18. R. Bai, G. He, L. Li, T. Zhang, J. Li, X. Wang, X. Wang, Y. Zou, D. Mei, A. Corma and J. Yu, *Angew. Chem. Int. Ed.*, 2023, **62**, e202313101.
19. M. Guo, H. Li, Y. Ren, X. Ren, Q. Yang and C. Li, *ACS Catal.*, 2018, **8**, 6476-6485.
20. K. Choe, F. Zheng, H. Wang, Y. Yuan, W. Zhao, G. Xue, X. Qiu, M. Ri, X. Shi, Y. Wang, G. Li and Z. Tang, *Angew. Chem. Int. Ed.*, 2020, **59**, 3650-3657.
21. R. Gao, J. Xu, J. Wang, J. Lim, C. Peng, L. Pan, X. Zhang, H. Yang and J. J. Zou, *J. Am. Chem. Soc.*, 2022, **144**, 573-581.
22. L. Zhao, X. Qin, X. Zhang, X. Cai, F. Huang, Z. Jia, J. Diao, D. Xiao, Z. Jiang, R. Lu, N. Wang, H. Liu and D. Ma, *Adv. Mater.*, 2022, **34**, 2110455.
23. H. Tian, F. Huang, Y. Zhu, S. Liu, Y. Han, M. Jaroniec, Q. Yang, H. Liu, G. Q. M. Lu and J. Liu, *Adv. Funct. Mater.*, 2018, **28**, 1801737.
24. Z. S. Wang, C. L. Yang, S. L. Xu, H. Nan, S. C. Shen and H. W. Liang, *Inorg. Chem.*, 2020, **59**, 5694-5701.